LASER
& PHOTONICS
REVIEWS

Laser Photonics Rev. **10,** No. 3, 441–450 (2016) / **DOI** 10.1002/lpor.201500256

**Abstract** Inspired from butterfly wings that exhibit unique dewetting properties and brilliant structural color synchronously, we reported here the preparation of biomimetic few-layer graphene films through a template-directed chemical vapor deposition method using laser-structured Cu foil as substrates. Hierarchical micronanostructures, including microscale stripes derived from the laser scanning and nanoscale laser-induced periodic surface structures (LIPSS), formed on Cu foil after a simple femtosecond laser treatment. By tuning the laser power, the surface roughness of the resultant Cu foils can be well controlled. Using the laser structures Cu foil as templates, biomimetic few-layer graphene films with both iridescence and superhydrophobicity have been successfully prepared. The present work may open up a new way to design and prepare structured graphene film in a biomimetic manner, and we deem that the bioinspired few-layer graphene films may find broad applications in the near future.

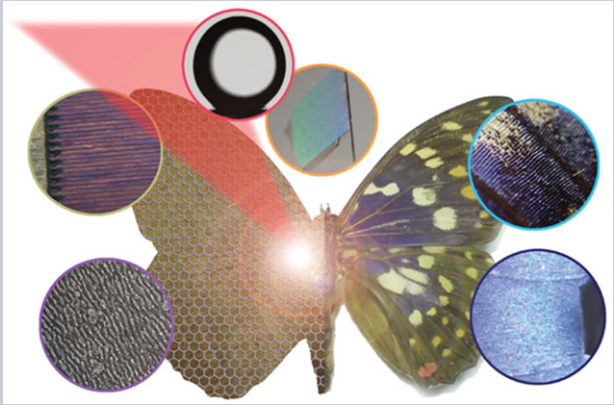

ORIGINAL
PAPER

# Bioinspired few-layer graphene prepared by chemical vapor deposition on femtosecond laser-structured Cu foil

**Hao-Bo Jiang[1], Yong-Lai Zhang[1,*], Yan Liu[3], Xiu-Yan Fu[1], Yun-Fei Li[1], Yu-Qing Liu[1], Chun-Hao Li[1], and Hong-Bo Sun[1,2,*]**

## 1. Introduction

After billions of years of evolution, natural creatures possess almost perfect micronanostructures and promising functions, for instance, the famous lotus leaf shows superhydrophobicity and a self-clean capability; butterfly wings, bird feathers and rose petals exhibit unique surface dewetting properties and beautiful structural color, all of these features could be attributed to the presence of multiscale micronanostructures [1]. The fascinating properties of natural materials continuously inspire scientists and engineers to design and fabricate artificial materials with hierarchical structures that mimic biomaterials towards multifunction integration [2], In the past few decades, bioinspired structures based on a wide range functional materials, for instance, polymers [3], metal oxides [4], carbon [5], and protein [6], have been successfully developed with the help of classical micronanofabrication techniques, represented by "top-down" and "bottom-up" approaches [7, 8]. For instance, laser processing has been widely employed to fabricate biomimetic superhydrophobic surfaces based on silicon [9,10]. However, in the pursuit of novel multifunctional devices with properties that rival those of natural materials, continued efforts in developing multiscale structures based on novel materials in a biomimetic manner are still highly desired.

Recently, a single-atom thick carbon crystal, named graphene, has attracted enormous research interests in various scientific fields, since it reveals a series of outstanding physical/chemical properties, such as ultrahigh carrier mobility [11], high thermal conductivity [12], high Young's modulus [13], optical transmittance [14], high electrical conductivity [15], flexibility [16], excellent stability [17] and biocompatibility [18]. Based on these intrinsic superiorities, graphene has already proved its value in various functional devices ranging from field-effect transistors (FETs) [19], optoelectronic devices [20] to smart actuators [21], demonstrating great potential for future electronics. To date, although graphene and its related materials have already revealed a cornucopia of both new physics and potential applications, scientific exploration of their full potential through rational design of their micronanostructures never stops. From this point of view, a flexible combination of graphene with bioinspired multiscale structures is undoubtedly a shortcut to reach this end. However, at present, biomimetic graphene is still at an early stage. In most cases, biomimetic graphene was prepared using graphene oxides (GO) as starting materials, since

[1] State Key Laboratory on Integrated Optoelectronics, College of Electronic Science and Engineering, Jilin University, 2699 Qianjin Street, Changchun 130012, China
[2] College of Physics, Jilin University, 119 Jiefang Road, Changchun 130023, China
[3] Key Laboratory of Bionic Engineering (Ministry of Education), Jilin University, Changchun 130022, China
*Corresponding author(s): e-mail: yonglaizhang@jlu.edu.cn, hbsun@jlu.edu.cn

chemically exfoliated GO not only allows mass production, but also shows tractable solution-processing capability [22]. More importantly, the presence of oxygen-containing groups (OCGs) on GO sheets permits flexible postfunctionalization by covalent grafting, which directly provides an opportunity for tuning the chemical composition on GO surfaces [23]. As typical examples, we fabricate superhydrophobic graphene surfaces that mimic rose petals and butterfly wings by means of a two-beam laser interference treatment of GO [24]. Inspired from nacre, An et al. prepared borate-crosslinked GO films with improved excellent mechanical strength by a simple cofiltration of GO solution and sodium tetraborate in combination with low-temperature annealing [25]. However, GO does not mean graphene; after drastically oxidation, residual OCGs dramatically alter the structure of the carbon plane. Even after a suitable reduction treatment, the presence of intrinsic defects all over the GO sheets significantly limits their further applications, especially for electronics.

Nowadays, the rapid progress of chemical vapor deposition (CVD) methods contributes to the production of high-quality and large-area graphene film on Cu or Ni substrates [26], which make it possible to prepare functional graphene structures on prestructured metal substrates. For instance, Yoon et al. fabricated a bioinspired graphene with dewetting property through a CVD method based on reconstructed Cu substrates that was prepared by simple heating of commercial Cu foil under different atmospheres [27]. Besides, Chen et al. reported the preparation of 3D graphene foam via CVD growth on Ni foam [28]; Wang et al. synthesized 3D graphene with improved electrochemical properties on a thick nickel foil using a microwave plasma CVD method [29]. Stratakis et al. reported a solution-based methodology for the preparation of free-standing few-layer graphene flakes on structured Si substrates [30]. However, all of these methods suffer from poor controllability over the formation of micronanostructures on Cu or Ni substrates; as a result, considerable difficulties arise when structuring the resultant graphene films into desired morphologies, not to mention mimicking biomaterials. Currently, it is still a big challenge to prepare biomimetic graphene through a template-directed CVD method towards exquisite control of their multiscale structures.

In this study, we report the fabrication of hierarchically structured few-layer graphene film that mimics butterfly wings using a template-directed CVD method. Femtosecond laser pulsing has been adopted for making multiscale structures on Cu foil, including microscale stripes derived from the laser scanning and laser-induced periodic surface structures (LIPSS) originated from the optical interference between the incident laser radiation and a surface electromagnetic wave (SEW). Using the structured Cu foil as template, few-layer graphene films that retain the structural features of the Cu substrates have been successfully prepared through a CVD method. Interestingly, the resultant few-layer graphene film demonstrates both superhydrophobicity and beautiful structural color, similar to that of butterfly wings.

## 2. Experimental

*Femtosecond laser processing of Cu foil*: A sapphire femtosecond laser amplifier (Spectra-Physics) with 800 nm center wavelength, 100 fs pulse duration, and 1 kHz repetition rate was used in our experiments. The direction of the laser polarization vector was changed by a half-wave plate. The laser spot is focused to 260 $\mu$m through a lens with a 600-mm focal distance, and the line scanning speed was 1 mm/s, so that each spot receives an average number of 260 pulses. Copper foil (99.9% purity, 25 $\mu$m thick) with a size of 25 mm $\times$ 25 mm were polished mechanically and cleaned ultrasonically in ethanol before laser treatment. Typically, the Cu foil was fixed on the receiving screen, which was mounted on a computer-controlled two-dimensional translation stage. In this way, the Cu foil was irradiated by the focused laser in a scanning manner. After laser treatment, LIPSS formed on the surface due to the coherent superposition effect between the incident wave of the laser and its scattered wave [31]. The resultant laser-structured Cu foil was denoted as Cu-*x*, where *x* is the laser power, Cu-50 mW means the Cu foil has been treated under a 50-mW femtosecond laser.

*CVD preparation of few-layer graphene on laser-structured Cu foil*: Laser-structured Cu foil was directly used for CVD growth of few-layer graphene without further treatment. In our work, CVD experiments were carried out at 1020°C in a furnace with a 22-mm inner diameter fused silica tube under ambient pressure. In the heating process, the flow rate of Ar was maintained at 300 SCCM and the flow rate of $H_2$ was maintained at 30 SCCM (SCCM denotes cubic centimeter per minute at STP). It takes 40 min to rise to the target temperature and then spends 30 min at that temperature. Then, the flow of hydrogen was shut off to produce an atmospheric flow in the quartz tube for 5 min. When the reaction process begins, 20 SCCM of $H_2$ and 2 SCCM of $CH_4$ were adopted as the carbon source. After reaction for 30 min, a few-layer graphene film on Cu foil was successfully prepared. To remove the Cu substrates, the samples were etched in $FeCl_3$/ HCl solution (1 M $FeCl_3$, 0.5 M HCl) for 6 h. The structured few-layer graphene film could be easily removed and transferred to any substrates, revealing that it is of good structural integrity. The resultant structured graphene was denoted as G-*x*, where *x* is the laser power used for Cu structuring, G-50 mW means the graphene film was prepared using Cu-50mW as a template.

*Characterization*: The CA measurements were implemented using the contact angle system OCA 20 (DataPhysics Instruments GmbH, Germany) at ambient temperature. The CAs were measured by the sessile-drop method with a water droplet of 4 $\mu$L. SEM images were obtained using a field-emission scanning electron microscope (JSM-7500F, JEOL, Japan). Atomic force microscopy (AFM) micrographs were obtained using a NanoWizard II BioAFM instrument (JPK Instruments AG, Berlin, Germany) in the tapping mode. Raman spectra were measured with a Renishaw Raman microscope using a 514-nm wavelength laser.

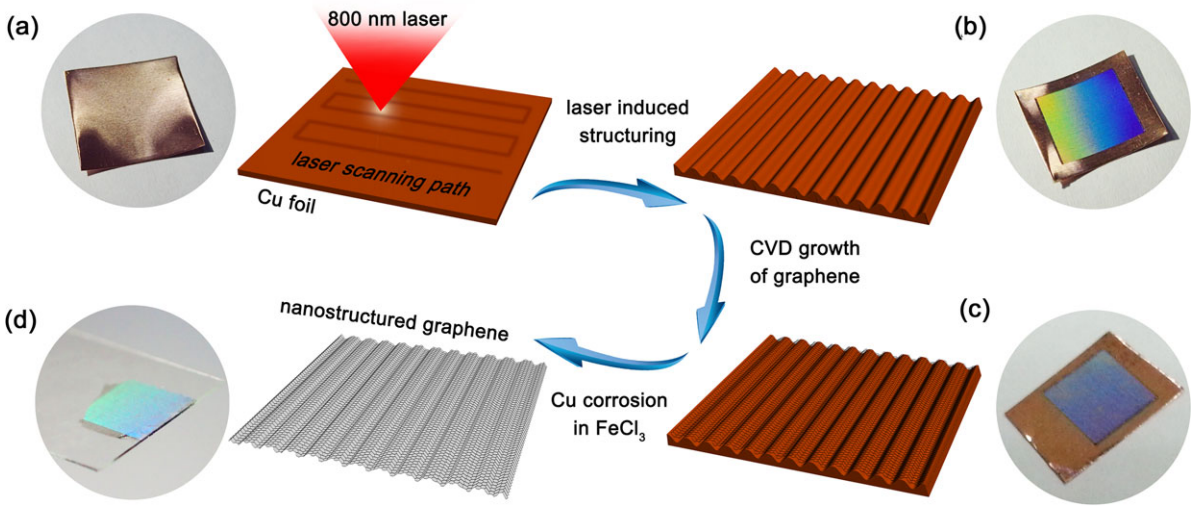


**Figure 1** Schematic illustration of the fabrication of butterfly-wing-inspired graphene films by template-directed CVD growth on femtosecond laser-structured Cu foil. (a) Photograph of a neat Cu foil used for laser structuring, a femtosecond laser pulse with a central wavelength of 800 nm was used for the experiments. (b) Photograph of a laser-structured Cu foil with structural color. (c) CVD growth of graphene on the laser-structured Cu foil. (d) The Cu foil has been etched in $FeCl_3$ solution, and the structured graphene film has been transferred to a cover glass.

## 3. Results and discussion

### *3.1. Fabrication of LIPSS on Cu foil*

To prepare biomimetic graphene film via a CVD method, flexible structuring of Cu or Ni substrates as templates to direct subsequent graphene growth is an essential step [31]. Typically, Cu foil has been widely recognized as a suitable substrate for CVD preparation of graphene. To date, there already exist abundant successful examples. To reproduce the hierarchical micronanostructures of typical butterfly wings on Cu foil, femtosecond laser processing has been used for making LIPSS that mimic butterfly wings through a mask-free and chemical-free manner. Figure 1 shows the diagrammatic sketch and relative photographs of the fabrication procedure. In a typical experiment, Cu foils (25 $\mu$m) with dimensions of 20 mm $\times$ 20 mm were mounted on a computer controlled two-dimensional translation stage, which guides the linear scanning by pulsed laser irradiation. The laser spot is estimated to be 260 $\mu$m and the scanning speed was 1 mm/s. In this way, the processing of a square (10 mm $\times$ 10 mm) could be accomplished within 25 min. Interestingly, after laser irradiation, the laser-scanned region of the Cu foil demonstrates brilliant iridescence (Fig. 1b), similar to those in butterfly wings and bird feathers. This directly suggests that LIPSS may be formed on the Cu foil. The spontaneous formation of LIPSS has been studied extensively for decades [32]. Generally, two types of LIPSS have been observed upon irradiation with multiple linearly polarized femtosecond-laser pulses, in which low spatial frequency LIPSS (LSFL) with spatial periods slightly smaller than or comparable to the laser irradiation wavelength is widely accepted [33]. The formation of LSFL is induced by the optical interference of the incident laser radiation with a surface electromagnetic wave (SEW), generated on the rough surface during the laser irradiation [34]. This theory may well explain the mechanism of formation of the LIPSS observed on the copper surfaces. Using the Cu foil with LIPSS as template, few-layer graphene could be prepared through a CVD method. After the growth of graphene film on the structured Cu substrates at 1000°C, the structural color still exists (Fig. 1c), indicating the formation of structured graphene. To get pure graphene film, the Cu substrates could be etched in $FeCl_3$/HCl solution, in this way, the structured graphene film could be transferred to any substrate. Notably, the resultant few-layer graphene film on a cover glass also demonstrates brilliant iridescence, which confirms the presence of periodic nanostructures on the graphene film (Fig. 1d).

To make an intuitionistic comparison between the hierarchical structures on a butterfly wing and our laser-structured Cu foil, we used confocal laser scanning microscopy (CLSM) to investigate their surface structures. Figure 2a shows the high-resolution photograph of the wing of an empress butterfly (inset of Fig. 2a), in which microscale stripes could be directly observed. When we observed the structures in the region of blue color by CLSM, we found that the stripes were constructed by the overlapping of arched scales with a size of about 100 $\times$ 150 $\mu$m, in this case, the period of the microstripe could be established to be $\sim$150 $\mu$m (Fig. 2b). A further magnified CLSM image shows that on each scale, there existed periodically distributed gratings with a period of $\sim$600 nm (Fig. 2c). The presence of such nanostructures is considered as essential to the structural color. For comparison, we also observed our laser-structured Cu foil by both camera and CLSM. As shown in Figs. 2d–f, after laser scanning, microscale stripes have also been observed from high-resolution

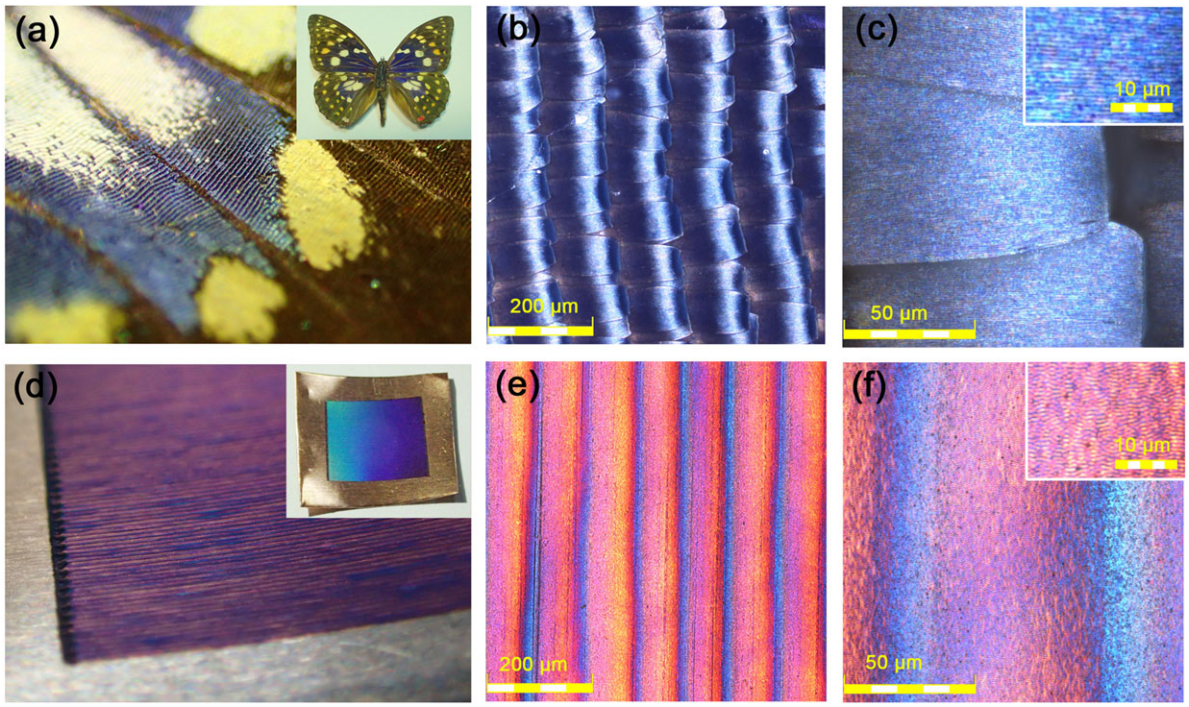


**Figure 2** Comparison of the hierarchical micronanostructures between natural butterfly wings and femtosecond laser-structured Cu foil. (a) Photograph of a butterfly wing, the inset is the photograph of the entire butterfly. (b) LSCM image of the microstructures of the butterfly wing. (c) Magnified LSCM image of a few scales on the wing, the inset shows the detailed nanostructures. (d) Photograph of a laser-structured Cu foil, the inset is the photograph of the entire Cu foil. (e) LSCM image of the microstructures of the laser-structured Cu foil. (f) Magnified LSCM image of laser-structured Cu foil, the inset shows the detailed nanostructures.

photograph; and the structured region shows beautiful structural color. The LSCM image shows that the period of microstripes formed by laser scanning is about 100 $\mu$m (Fig. 2e). The magnified CLSM image reveals that LIPSS formed on the surface (Fig. 2f). The formation of LIPSS accounts for the presence of iridescence on the Cu foil (inset of Fig. 2d). From the comparison, it can be found that the microstripes in combination with LIPSS on the Cu foil are quite similar to the hierarchical structures on butterfly wings. Using this laser-structured Cu foil as a template, the preparation of biomimetic graphene film could be expected.

In fact, the formation of ripple structures is dominated by both exposure conditions and material properties. For instance, the obtained ripple structures further depend on a series of parameters that are proportional to the pulse energy, including the fluence per pulse, the spatial intensity distribution, a cumulative exposure dose (number of pulses), thus some laser parameters have to be optimized to create LIPSS [35,36]. In our work, the pulse duration, pulse number, polarization, and the irradiation wavelength have been fixed, so the period of ripples on the laser-structured Cu foil show a similar value. To get better control over the surface topologies of the laser-structured Cu foil, we tuned the fluence within a certain range to alter the surface roughness by introducing microscale particles. It is known that the single pulse energy and the number of laser pulses per irradiation spot $N$ can significantly affect the formation of LIPSS [37]. Generally, $N$ can be defined by the following equation:

$$N = f/(z * v),$$

where $f$ is the laser repetition rate; $z$ is the laser scanning line spacing; and $v$ is the laser scanning speed [38]. According to this equation, $N$ has a fixed value of $1.67\times10^6$ /cm$^2$. Hence, we tuned the laser power (50, 100, 150, 200 mW) to process the Cu foil. Since the repetition rate is fixed at 1 kHz, the corresponding single pulse energy is calculated to be 50, 100, 150, and 200 $\mu$J, respectively.

Figure 3 shows the SEM images of the LIPSS on the Cu foils fabricated under different laser powers. It can be clearly identified from the SEM image that periodic ripples formed all over the laser-irradiated region, indicating the formation of LIPSS. The period was measured to be ~600 nm, which is smaller than that of the laser wavelength (800 nm). Actually, a special fluence regime, namely, near-damage-threshold fluence, was required for the formation of LIPSS [39]. According to our results, the threshold laser fluence was ~80 J/cm$^2$. Notably, when the incident laser power is 50 mW (Figs. 3a and b), the laser fluence was evaluated to be $6.37\times10^5$ mJ/cm$^2$. In this case, the periodic ripples are very clear. With the increase of laser power, the period of the ripple maintains a consistent value of ~600 nm, which is in good agreement with the formation principle discussed above. When we increased the laser

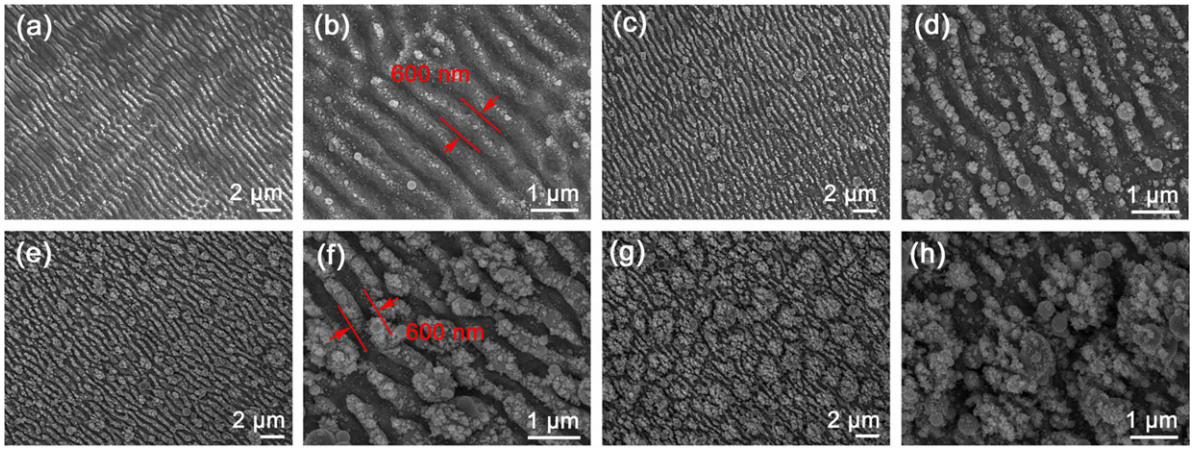


**Figure 3** SEM images of laser-structured Cu foils prepared under different laser fluences. (a, b) Cu-50mW (laser fluence: $6.37\times10^5$ mJ/cm$^2$), (c, d) Cu-100mW (laser fluence: $12.74\times10^5$ mJ/cm$^2$), (e, f) Cu-150mW (laser fluence: $19.11\times10^5$ mJ/cm$^2$) and (g, h) G-200mW (laser fluence: $25.48\times10^5$ mJ/cm$^2$).

fluence to $19.11\times10^5$ mJ/cm$^2$ (Figs. 3c and d), a few nanoparticles form by redeposition. Further increase of laser fluence would result in the formation of more particles on the surface, making the Cu substrates very rough (Figs. 3e–h). The formation of Cu islands could be attributed to the reflow and redeposition of ablated Cu particles at high laser fluences, which is very common in the cases of laser-structured metallic and semiconducting surfaces [9, 10]. To get more information about the particles formed at high laser fluence, XPS and XRD characterization has been carried out based on the high laser fluence sample (200 mW), which indicate that copper has been slightly oxidized in the processing conditions (for details, see supporting information Fig. S1). However, in the XRD patterns (Fig. S2), the Cu oxide-related peaks were absent, indicating that the oxide layer is very thin. We have to point out that the Cu oxide layer could be fully reduced to Cu before the growth of graphene, since a $H_2$ annealing has been implemented before the introduction of the carbon source ($CH_4$).

### *3.2. CVD preparation of biomimetic few-layer graphene film*

Using the laser-structured Cu foil as template, few-layer graphene film could be readily prepared via a CVD process. Interestingly, as shown in Figs. 1c and d, both the Cu foil with graphene and the resultant graphene layer that has been transferred to a cover glass demonstrate beautiful structural color, which indicates the presence of similar nanostructures. In order to investigate the morphology change before and after CVD process, we compared the same Cu foil surface before and after CVD process by AFM (Fig. S3). The morphologies of these laser-structured Cu foils do not show any obvious change after CVD growth of graphene. The height of ripples decreased after CVD; and the average roughness of the four samples slightly decreased (Fig. S4), which could be attributed to the Cu reflow and copper oxide reduction at high temperature. To gain further insight into the surface structure of the as-obtained few-layer graphene, SEM and AFM have been used to characterize the samples prepared using different Cu foils as templates. Figure 4 shows the SEM images of the boimimetic few-layer graphene films. Inherited from the nanostructures on Cu foil, the resultant few-layer graphene film also demonstrates similar nanostructures, nanoripples with a period of ~600 nm could be clearly identified from the surface (Fig. 4b). The periodic nanoripples account for the formation of structural color. Similar to structures on Cu foil, nanoparticles formed with the increase of laser power. Using Cu-100mW as template, a few nanoparticles appear on the nanoripple structure (Fig. 4b). The CLSM image confirms the large-area nanoripple structure (Fig. 4c). When we use the rough Cu foil prepared under higher laser power (e.g., 150 mW and 200 mW), the resultant few-layer graphene films become rougher (Figs. 4d and e). Plenty of particles formed between the nanoripple structures, which is quite similar to the morphology of laser-structured Cu foil. By carefully observing the particles, we found some wizened graphene shells, as shown in the inset of Fig. 4e. The formation of such wizened graphene shells could be atrributed to the etching of Cu particles. As typical examples, we also observed the roughest few-layer graphene film by CLSM. As shown in Fig. 4f, both the microstripes and the nanoripple structures that are similar to LIPSS on Cu foil have been observed. In addition, we also investigate the thickness of the obtained few-layer graphene film by TEM. According to the cross-sectional TEM image shown in Fig. S5 (supporting information), the as-formed graphene film was about 5–10 layers. In this regard, it is more appropriate to refer to our material as few-layer graphene.

To get furhter insight into the surface structures of the resultant biomimetic few-layer graphene films, the four samples have been characterized by AFM. Interestingly, the AFM patterns (Fig. 5) are quite similar to that shown in SEM images (Fig. 4). Take G-50 mW as an example, the height profile along the white line of Fig. 5a shows that

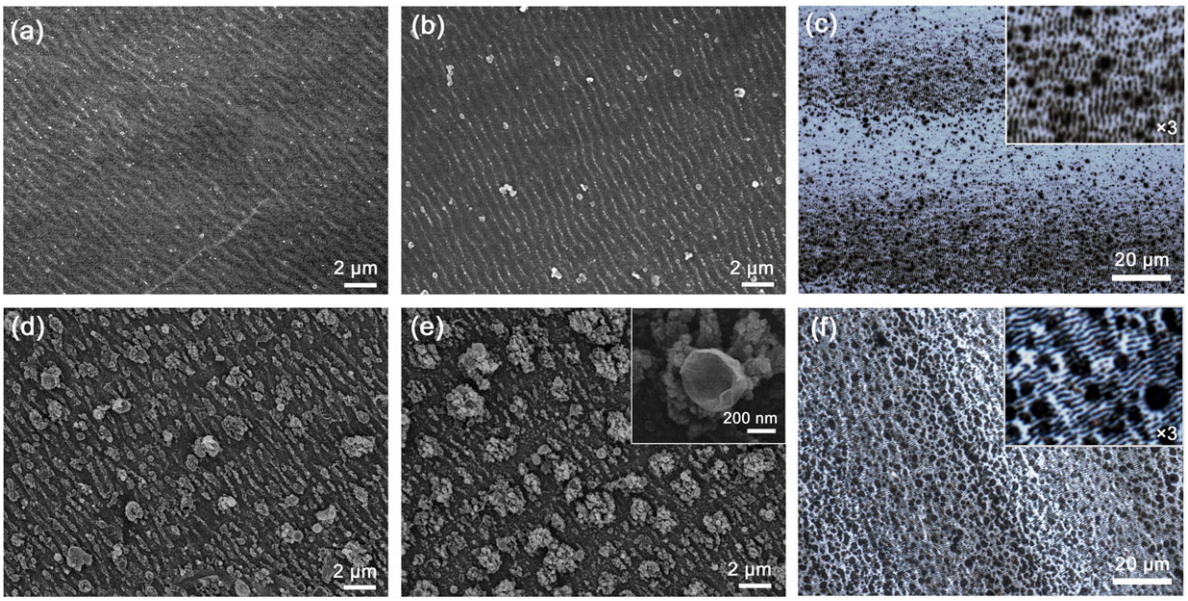


**Figure 4** SEM images of micronanostructured graphene films prepared by CVD using different laser-structured Cu foils as templates. (a, b, d, e) Micronanostructured graphene films (a) G-50mW (laser fluence: $6.37\times10^5$ mJ/cm$^2$), (b) G-100mW (laser fluence: $12.74\times10^5$ mJ/cm$^2$), (d) G-150mW (laser fluence: $19.11\times10^5$ mJ/cm$^2$) and (e) G-200mW (laser fluence: $25.48\times10^5$ mJ/cm$^2$). (c) CLSM image of G-100mW, the inset is detailed nanostructures magnified by 3 times. (f) CLSM image of G-200mW, the inset is detailed nanostructures magnified by 3 times.

the period is ~600 nm, and the height of the structure is ~20 nm. With increasing laser power, the period of the LIPSS maintains a consistent value, whereas the height of the structures slightly increases. Figure 5b shows the AFM image of G-100 mW, the period is also ~600 nm, but the height of the structure increases to ~200 nm. Further increase of the laser power would lead to the formation of rough surfaces, as shown in Figs. 5c and d. LIPSS with a period of ~600 nm could still be observed, the height of the structure increased to ~300 and ~400 nm, respectively. Generally, the Cu foil treated under lower laser power demonstates fine LIPSS structure, and the resultant few-layer graphene film also shows similar mophology. In this case, the surface is quite flat. On the contrary, the increase of laser power would lead to more rough structures on Cu foil, and the resultant few-layer graphene film is also very rough. Form this point of view, the surface roughness could be tuned by changing the laser power during the structuring of Cu foil. It is well known that the surface dewetting property is highly depended on roughness [40], precise control of the surface roughness of the resultant few-layer graphene films would lead to tunable surface wettabilities.

### 3.3. Characterization of structured few-layer graphene films

It is well known that Raman spectroscopy has been widely used for characterizing the hybrid nature of carbon materials [41]. In our work, Raman spectra have been collected to evaluate the structure of the resultant few-layer graphene films, as shown in Fig. 6a. Obviously, the Raman spectra of our few-layer graphene films display two peaks at 1340 cm$^{-1}$ and 1600 cm$^{-1}$, which correspond to *D* and *G* band, respectively [41]. The *G* band is attributed to an $E_{2g}$ mode of graphite associated with the vibration of sp$^2$-bonded carbon atoms, whereas the *D* band peak is related to the oscillations of carbon atoms with dangling bonds in plane terminations of disordered graphite [42]. The presence of the *D* band could be attributed to defects. For the four few-layer graphene samples, the intensity ratio of *D* band and *G* band, $I_D/I_G$, slightly increased from 0.91 to 0.95, which indicates the rough Cu foil would generate more defects. Additionally, the Raman spectra show a very broad 2D peak in the range of 2500–3000 cm$^{-1}$. To gain further insight into the 2D region, the broad 2D peak of 200 mW sample was fitted using Lorentzian profiles. As shown in the inset of Fig. 6a, the broad region was composed of multiple peaks of 2D, D+G and 2D′ at 2685, 2930 and 3150 cm$^{-1}$, respectively. The presence of D+G and 2D′ peaks could be attributed to the nonplanar feature of our structured few-layer graphene layers. These characteristics of Raman can be easily found in nanostructured or curved graphene as reported elsewhere [43, 44].

Figure 6b shows optical transmittance spectra of our biomimetic few-layer graphene films. In our work, G-50mW sample has a transmittance of ~71.5% when the incident laser wavelength is 500nm. The transmittance of G-100mW, G-150mW and G-200mW samples decreased to ~68.5%, ~63.9%, ~57.1%, respectively, when relative

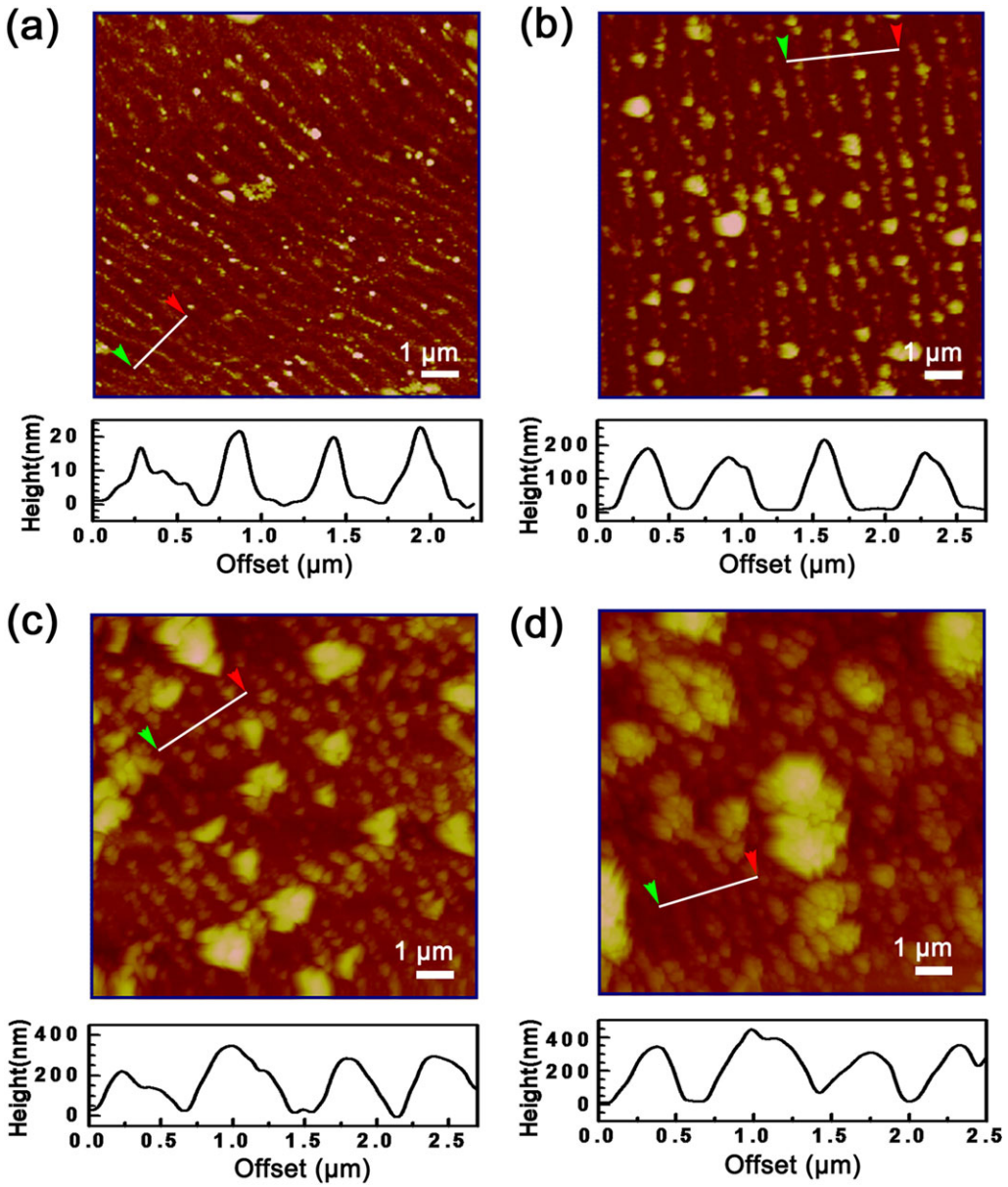


**Figure 5** AFM images (upper images) and height profiles (bottom images) of micronanostructured graphene films (a) G-50mW (laser fluence: $6.37\times10^5$ mJ/cm$^2$), (b) G-100mW (laser fluence: $12.74\times10^5$ mJ/cm$^2$), (c) G-150mW (laser fluence: $19.11\times10^5$ mJ/cm$^2$) and (d) Gu-200mW (laser fluence: $25.48\times10^5$ mJ/cm$^2$).

rough Cu foils were used as templates. Such transmittance in the visible-light range could guarantee the transparent property, as shown in the inset of Fig. 6b.

### *3.4. Wetting properties and optical performance*

Generally, two factors influent the wettability of solid surface, one is surface microstructures, and the other is the surface chemical composition [45]. Due to the high surface free energy of copper and copper oxide, the polished copper surface shows a hydrophilic property, whereas the laser-structured Cu surfaces show a contact angle (CA) of ~90º. The growth of graphene on the surface of Cu significantly altered the surface energy, since graphene has relative low surface free energy [46]. Here, to quantificationally investigate superhydrophobicity of the micronanostructured few-layer graphene films, a static water CA measurement has been carried out on these four kinds of few-layer graphene films. As shown in Fig. 7, all of the microstructured few-layer graphene films show hydrophobicity, generally, with a CA value in the range of 106–152°. The presence of hierarchical micronanostructures has been considered to be an essential factor to gain the hydrophobicity. In particular, when the laser intensity is as high as 200 mW, the Cu-200mW sample is very

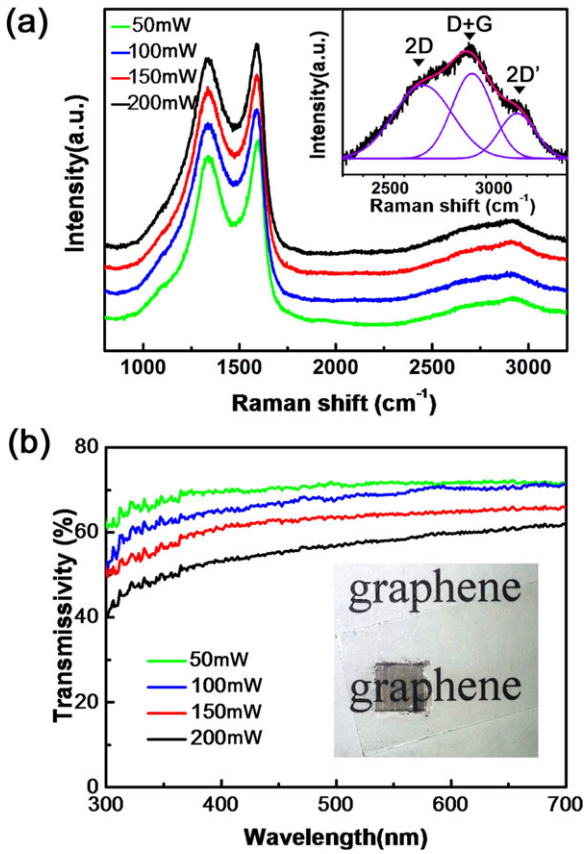


**Figure 6** (a) Raman spectra and (b) optical transmission spectra of micronanostructured graphene films prepared by CVD growth on different Cu foils. The inset of (a) shows the 2D region fitted using Lorentzian profiles. The inset of (b) is the photograph of a graphene film (Cu-200mW as template), which has been transferred to a glass slide. Laser power of 50, 100, 150 and 200 mW corresponds to laser fluences of $6.37\times10^5$, $12.74\times10^5$, $19.11\times10^5$ and $25.48\times10^5$ mJ/cm$^2$, respectively.

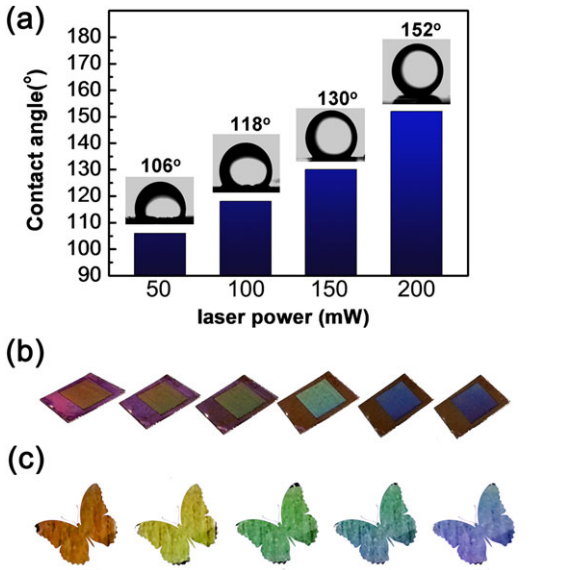


**Figure 7** (a) Static water droplet CAs of micronanostructured graphene films prepared by CVD growth on different templates. The insets are photographs of a water droplet on corresponding surfaces. Laser powers of 50, 100, 150 and 200 mW correspond to laser fluences of $6.37\times10^5$, $12.74\times10^5$, $19.11\times10^5$ and $25.48\times10^5$ mJ/cm$^2$, respectively. (b) Photographs of Cu-200mW foil after CVD growth of a graphene film on the surface. (c) Structural color of the micronanostructured graphene film (Cu-200mW as template), which has been transferred to a glass slide.

rough, containing both nanoripples and the nanoparticles. In this case, the resultant G-200mW shows the highest CA of 152°, reaching the superhydrophobic level. The ripple structures shows the certain influence on the anisotropic wettability of the surface, we measured the CA and sliding angle (SA) from the orthogonal and parallel direction, respectively (Figs. S6 and S7). The CA measured from the orthogonal direction is slightly higher than that from the parallel direction. We also measured the SA of the superhydrophobic sample G-200mW. The SA measured from the orthogonal and parallel direction were measured to be 8° and 6°, respectively, indicating the Cassie superhydrophobic state.

Similar to the brilliant butterfly wings, when light irradiates on the biomimetic few-layer graphene films, structural color could be clearly observed [47]. The structural color could be attributed to the diffraction of the LIPSS, expressed as the following equation:

$$m\lambda = d(\sin\theta_D - \sin\theta_I),$$

where $m$ is the diffraction order, $d$ is the period of the grating, and $\theta_D$ and $\theta_I$ are the diffraction and incident angles, respectively [48]. Notably, light of a different wavelength diffracted when changing the viewing angle, and beautiful structural color could be observed due to the chromatic dispersion. Figure 7b shows iridescence of few-layer graphene on Cu foil without corrosion. Figure 7c explored iridescence of few-layer graphene on glass substrates that were captured by camera. With the increase of laser fluence, the resultant few-layer graphene samples all show structural color due to the presence of ripple structures.

## 4. Conclusion and outlook

Inspired from butterfly wings, hierarchically structured few-layer graphene films that feature unique superhydrophobicity and brilliant structural color have been successfully prepared by using a template-directed CVD method. Femtosecond-laser processing has been adopted for the structuring of Cu foil. Without any masks, hierarchical structures including microscale stripes and nanoscale LIPSS have been successfully fabricated due to the laser scanning and the optical interference between the incident laser and a SEW. Inherited from the multiscale structures on Cu foil, few-layer graphene film prepared by CVD could be transferred from the Cu foil to any substrate and well retained the hierarchical structures, demonstrating both the

dewetting property and iridescence, similar to those of butterfly wings. Notably, ultrafast laser processing is capable of making surface micronanostructures on active metal substrates [49] (e.g., Cu and Ni) that are suitable for graphene preparation. With the rapid progress of CVD technologies, high-quality graphene with desired micronanostructures could be readily prepared by using laser-structured Cu foils as templates. As a typical example, the biomimetic graphene films hold great promise for various potential uses in organic light-emitting diodes (OLEDs) and organic solar cells (OSCs). By designing different surface micronanostructures on Cu foil, structured graphene may find more applications in both fundamental science and practical usage.

## Supporting Information

Additional supporting information may be found in the online version of this article at the publisher's website.

**Acknowledgements.** The authors would like to acknowledge the National Natural Science Foundation of China (NSFC) and National Basic Research Program of China under grants #61522503, #61590930, #2011CB013000, #61376123, and #61435005) for support.

**Received:** 12 October 2015, **Revised:** 21 December 2015, **Accepted:** 18 February 2016

**Published online:** 14 March 2016

**Key words:** Bioinspired structures, graphene, CVD, laser processing, superhydrophobic surface.

## References

[1] C. Sanchez, H. Arribart, and M. M. G. Guille, Nature Mater **4**, 277–288 (2005).
[2] K. Liu and L. Jiang, Nano Today **6**, 155–175 (2011).
[3] K. Liu, Y. Tian, and L. Jiang, Prog. Mater. Sci. **58**, 503–564 (2013).
[4] Z. Y. Zhang, J. D. Huang, B. Dong, Q. Yuan, Y. Y. He, and O. S. Wolfbeis, Nanoscale **7**, 4149–4155 (2015).
[5] J. N. Wang, R. Q. Shao, Y. L. Zhang, L. Guo, H. B. Jiang, D. X. Lu, and H. B. Sun, Chem. Asian J. **7**, 301–304 (2012).
[6] Y. L. Sun, W. F. Dong, R. Z. Yang, X. Meng, L. Zhang, Q. D. Chen, and H. B. Sun, Angew. Chem. Int. Ed. **51**, 1558–1562 (2012).
[7] S. G. Zhang, Nature Biotechnol. **21**, 1171–1178 (2003).
[8] K. H. Smith, E. Tejeda-Montes, M. Poch, and A. Mata, Chem. Soc. Rev. **40**, 405–415 (2011).
[9] T. Baldacchini, J. E. Carey, M. Zhou, E. Mazur, Langmuir **22**, 4917–4919 (2006).
[10] V. Zorba, E. Straakis, M. Barberoglou, E. Spanakis, P. Tzanetakis, P. H. Anastasiadis, and C. Fotakis, Adv. Mater. **20**, 4049–4054 (2008).
[11] J. C. Meyer, A. K. Geim, M. I. Katsnelson, K. S. Novoselov, T. J. Booth, and S. Roth, Nature **446**, 60–63 (2007).
[12] I. Calizo, A. A. Balandin, W. Bao, F. Miao, and C. N. Lau, Nano Lett. **7**, 2645–2649 (2007).
[13] C. Lee, X. D. Wei, J. W. Kysar, and J. Hone, Science **321**, 385–388 (2008).
[14] S. Bae, H. Kim, Y. Lee, X. Xu, J.-S. Park, Y. Zheng, J. Balakrishnan, T. Lei, H. R. Kim, Y. I. Song, Y.-J. Kim, K. S. Kim, B. Ozyilmaz, J.-H. Ahn, B. H. Hong, and S. Iijima, Nature Nanotechnol. **5**, 574–578 (2010).
[15] Y. Zhang, Y.-W. Tan, H. L. Stormer, and P. Kim, Nature **438**, 201–204 (2005).
[16] D. D. Han, Y. L. Zhang, H. B. Jiang, H. Xia, J. Feng, Q. D. Chen, H. L. Xu, and H. B. Sun, Adv. Mater. **27**, 332–338 (2015).
[17] C. O. Girit, J. C. Meyer, R. Erni, M. D. Rossell, C. Kisielowski, L. Yang, C.-H. Park, M. F. Crommie, M. L. Cohen, S. G. Louie, and A. Zettl, Science **323**, 1705–1708 (2009).
[18] Z. S. Qian, X. Y. Shan, L. J. Chai, J. J. Ma, J. R. Chen, and H. Feng, Nanoscale **6**, 5671–5674 (2014).
[19] H. G. Sudibya, Q. He, H. Zhang, and P. Chen, ACS Nano **5**, 1990–1994 (2011).
[20] H. Park, P. R. Brown, V. Bulovic, and J. Kong, Nano Lett. **12**, 133–140 (2012).
[21] L. Guo, H. B. Jiang, R. Q. Shao, Y. L. Zhang, S. Y. Xie, J. N. Wang, X. B. Li, F. Jiang, Q. D. Chen, T. Zhang, and H. B. Sun, Carbon **50**, 1667–1673 (2012).
[22] Y. L. Zhang, L. Guo, S. Wei, Y. Y. He, H. Xia, Q. D. Chen, and H. B. Sun, Nano Today 5 15–20 (2010).
[23] Y. L. Zhang, L. Guo, H. Xia, Q. D. Chen, J. Feng, and H. B. Sun, Adv. Opt. Mater. **2**, 10–28 (2014).
[24] H. B. Jiang, Y. L. Zhang, D. D. Han, H. Xia, J. Feng, Q. D. Chen, Z. R. Hong, and H. B. Sun, Adv. Funct. Mater. **24**, 4595–4602 (2014).
[25] Z. An, O. C. Compton, K. W. Putz, L. C. Brinson, and S. T. Nguyen, Adv. Mater. **23**, 3842 (2011).
[26] X. Li, X. B. Zang, Z. Li, X. M. Li, P. X. Li, P. Z. Sun, X. Lee, R. J. Zhang, Z. H. Huang, K. L. Wang, D. H. Wu, F. Y. Kang, and H. W. Zhu, Adv. Funct. Mater. **23**, 4862–4869 (2013).
[27] J. C. Yoon, C. S. Yoon, J. S. Lee, and J. H. Jang, Chem. Commun. **49**, 10626 (2013).
[28] Z. P. Chen, W. C. Ren, L. B. Gao, B. L. Liu, S. F. Pei, and H. M. Cheng, Nature Mater. **10**, 424–428 (2011).
[29] C. D. Wang, Y. Li, Y. S. Chui, Q. H. Wu, X. F. Chen, and W. J. Zhang, Nanoscale **5**, 10599 (2013).
[30] E. Stratakis, G. Eda, H. Yamaguchi, E. Kymakis, C. Fotakis, and M. Chhowalla, Nanoscale **4**, 3069 (2012).
[31] J. B. Sun, J. B. Hannon, R. M. Tromp, P. Johari, A. A. Bol, V. B. Shenoy, and K. Pohl, ACS Nano **12**, 7073–7077 (2010).
[32] Y. Y. Huo, T. Q. Jia, D. H. Feng, S. Zhang, J. K. Liu, J. Pan, K. Zhou, and Z. R. Sun, Laser Phys. **23**, 056101 (2013).
[33] J. Bonse, A. Rosenfeld, and J. Kruger, J. Appl. Phys. **106**, 104910 (2009).
[34] G.D. Tsibidis, E. Stratakis, P.A. Loukakos, and C. Fotakis, Appl. Phys. A: Mater. Sci. Process. **114**, 57–68 (2014).
[35] G. D. Tsibidis, M. Barberoglou, P. A. Loukakos, E. Stratakis, and C. Fotakis, Phys. Rev. B **86**, 115316 (2012).
[36] G. D. Tsibidis, C. Fotakis, and E. Stratakis, Phys. Rev. B **92**, 041405(R) (2015).

[37] J. Y. Long, P. X. Fan, M. L. Zhong, H. J. Zhang, Y. D. Xie, and C. Lin, Appl. Surf. Sci. **311**, 461–467 (2014).
[38] J. H. Zhao, C. H. Li, Q. D. Chen, and H. B. Sun, IEEE Sens. J. **15**, 4259 (2015).
[39] S. Nolte, C. Momma, H. Jacobs, A. Tunnermann, B.N. Chichkov, B. Wellegehausen, and H. Welling, J. Opt. Soc. Am. B **14**, 2716–2722 (1997).
[40] D. Wu, J. N. Wang, S. Z. Wu, Q. D. Chen, S. Zhao, H. Zhang, H. B. Sun, and L. Jiang, Adv. Mater. **21**, 2927–2932 (2011).
[41] A. Das, S. Pisana, B. Chakraborty, S. Piscanec, S. K. Saha, U. V. Waghmare, K. S. Novoselov, H. R. Krishnamurthy, A. K. Geim, A. C. Ferrari, and A. K. Sood, Nature Nanotechnol. **3**, 210–215 (2008).
[42] F. Tuinstra and J. L. Koenig, J. Chem. Phys. **53**, 1126 (1970).
[43] S. Lee, J. Hong, J. H. Koo, H. Lee, S. Lee, T. Choi, H. Jung, B. Koo, J. Park, H. Kim, Y. W. Kim, and T. Lee, ACS Appl. Mater. Inter. **5**, 2432−2437 (2013).
[44] S. Wang, X. Huang, Y. He, H. Huang, Y. Q. Wu, L. Z. Hou, X. L. Liu, T. M. Yang, J. Zou, and B. Y. Huang, Carbon **50**, 2119–2125 (2012).
[45] Y. L. Zhang, H. Xia, E. Kim, and H. B. Sun, Soft.Matter **8**, 11217 (2012).
[46] J. N. Wang, Y. L. Zhang, Y. Liu, W. H. Zheng, L. P. Lee, and H. B. Sun, Nanoscale **7**, 7101 (2015).
[47] O. Sato, S. Kubo, and Z. Z. Gu, Accounts Chem. Res. **42**, 1–10 (2009).
[48] J. W. Yao, C. Y. Zhang, H. Y. Liu, Q. F. Dai, L. J. Wu, S. Lan, A. V. Gopal, V. A. Trofimov, and T. M. Lysak, Appl. Surf. Sci. **258**, 7625–7632 (2012).
[49] A. Y. Vorobyev and C. L. Guo, Laser Photon. Rev. **7**, 358–407 (2013).